

Prediction of Solar Flares from a Statistical Analysis of Events during Solar Cycle 23

Z. Q. Qu¹, C. L. Xu³, X. L. Yan^{1,2}, Z.K.Xue^{1,2} and Z.N.Qu^{1,2}

ABSTRACT

Ways to give medium- and short-term predictions of solar flares are proposed according to the statistical analysis of events during solar cycle 23. On one hand, the time distribution of both C and M class flares shows two main periods of 13.2 and 26.4 months in this cycle by wavelet analysis. On the other hand, active regions of specific magnetic configurations and their evolutions give high productivity of C class flares but relatively low productivity of energetic (M and X class) flares. Furthermore, by considering the measurable kinetic features of active regions, i.e., the rotation of the sunspots, some active regions of specified types are observed to have high energetic flare productivity, above 66%. The periodicity of the activity revealed can be used for medium-term C and M class flare forecasting and the high productivity of active regions forms the basis for short-term prediction of individual energetic flares.

Subject headings: sun: flares prediction; sun: active regions; sun: sunspots

1. Introduction

Flare prediction is an emergent but very difficult task for solar physicists. Not only because the mechanisms involved in flare occurrence are complicated (Tandberg-Hansen and Emislie, 1988), but also the theories and observations are not very operationally related. It is now well known that the short-term prediction of individual flares should be done before or during the phase of magnetic energy storage resulting in the energy release later. Therefore, searching for sufficient or sufficient-like pre-flare conditions is more helpful than searching for necessary ones in this aspect. Statistical analysis is still a good tool to find such conditions,

¹Yunnan Astronomical Observatory, National Astronomical Observatories, Chinese Academy of Sciences, Kunming, Yunnan 650011, P.R. China.

²Graduate School of Chinese Academy of Sciences, Zhongguancun, Beijing, P.R. China.

³Yunnan Normal University, Kunming, Yunnan 650092, P.R.China.

and these sufficient or sufficient-like conditions must correspond to the emergence of some determinant features of active regions. In this paper, we try to find such conditions by the statistics of events during solar cycle 23.

Concerning the search for the pre-flare conditions, several ways were proposed by investigators in the literature. For instance, the most popular way is to find the correlations between sunspot magnetic features and major flares (e.g. Greatrix 1963; Mayfield and Lawrence, 1985; Atac 1987; Sammis et al., 2000; Ternullo et al., 2006). Based on this kind of correlation and solar cycle data, Qahwaji and Colak (2007) established an automatic short-term prediction system with an ability of machine-learning. On the other hand, some statistical correlation between flare productivity and more detailed magnetic features, like maximum horizontal gradient of photospheric vector magnetic fields, length of neutral lines, and number of singular points, as well as magnetic shear, has been done by Cui and Wang (2007), and Cui et al. (2007). They found the correlation can be fitted by Boltzmann sigmoid functions and proposed that this relationship can be used for modeling flare forecasting.

At the present stage, we are far from forecasting all the flares or even only significant flares individually. However, it is very useful to give medium- and short-term predictions of some individual energetic (M and X class) flares. This is the main purpose of this paper. Gallagher, Moon and Wang (2002) based on the flare productivity of active regions, proposed some kind of flare forecasting, giving even 10 variables including McIntosh classification, sunspot group area, the number of sunspots, the average hardness indexes, etc. in their model. Like Jakimiec and Bartkowiak (1994), other similar features were included (Zhu and Wang, 2003). However, the short-term prediction of a great number of individual flares is far from satisfactory (Zhu and Wang, 2003). Therefore, searching the determinant variables which promote the prediction is crucial. Another way was proposed by Wheatland (2001), that the rate of flare production in single active regions from 1981 to 1999 can be obtained by studying the waiting-time distribution (WTD) for individual regions and the relation reflecting WTD, say, described by Poisson process can be used for the prediction. Evidently these two methods are complementary and can be used for further investigations in this field.

2. Periodicity of Activity and High Flare Productivity Found during Solar Cycle 23

Solar cycle 23 provides some clues. Gaining some characteristics of this cycle can help us make the predictions for the next cycle. All of the data for the events used for our analysis stem from the website <http://www.solarmonitor.org/>. When counting flares, we should be careful to get rid of recounted flares recorded on the site in neighboring days. The time span

covers the whole of solar cycle 23, i.e., from Feb. 1996 to Jan.2008. The total number of flares recorded by the website is 21,620, while 19,577 flares were classified as C class, 1,887 as M class and 156 as X class according to soft X ray flux classification. There were 11,138 (10,516 C class, 587 M class and 35 X class) flares not related to numerated active regions. They are also included for the statistical analysis. In order to have an overview of these recorded flares, Fig.1 outlines the number distribution of the flares of different soft X ray flux. One can see that the M1 class of flares stands out as an exception and this may become a feature of the activity of the cycle . We use the exponential function

$$N(x) = a + be^{-c \log_{10} x} \quad (1)$$

to describe the number distribution (solid line), where x means the soft X ray flux irradiated by flares. The coefficients ($a = 76, b = 2.0 \times 10^{-5}, c = 4.07$) can become other characteristic quantities describing the activity of this cycle. In the fitting, we do not include either the faintest flares (C1.0) recorded, because the number of these flares are likely underestimated, or the highest energetic flares above X10.0 because they are very rare.

In the upper panel of Fig.2, the number evolution of events with solar flare classification is depicted. One can see that the pattern takes on periodicity except for X class flares, whose number evolution is not plotted individually. This stimulates us to use the wavelet analysis with the Marlet function as the wavelet function to find the periods. In the lower panel, the corresponding power spectra are shown. It is obvious that all the curves have two prominent peaks at the 13.2 and 26.4 months for both C class and M class flare occurrence, and finally for all the recorded flares. Furthermore, the phases are also very close to each other. Such periodicity can be used for medium-term prediction of the next cycle, although the periods cannot be expected to be same. Finally, we may assign these periods as features of this cycle.

It is generally accepted that special magnetic configurations and their evolution induce flare eruptions. At the present stage, the three dimensional classification is not at hand for all the numerated active regions and the two dimensional Hale and McIntosh classifications are more frequently used. The lower panel of Fig.3 presents the numbers of the active regions belonging to particular magnetic configurations (Hale classification) without any configuration variation within one day. A similar diagram also appeared in the work by Ternullo et al.(2006) but only into June 2003. In the following, the flare productivity is defined as the ratio of the number of active regions hosting flares of specific class to the total number of active regions of the same specified type. The configuration β is dominant in this cycle. However, the flare production does not favor of this configuration or another simple one, α . High flare productivity occurs in other configurations, i.e. $\beta\delta$ (64%, 25 regions hosting flares in 39 regions owned this configuration), $\beta\gamma$ (53%, 547 in 1033), $\beta\gamma\delta$ (75%, 300

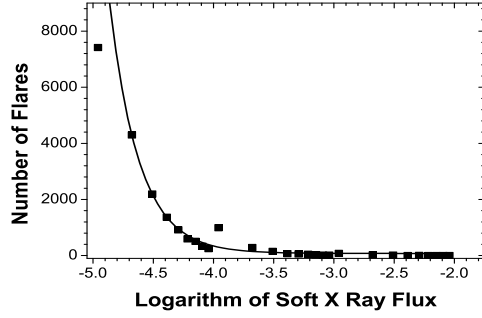


Fig. 1.— Number distribution of flares to logarithm of soft X ray flux irradiated by flares in unit of erg/cm²s. The solid line is the fitting by Eq.(1) as stated in the text.

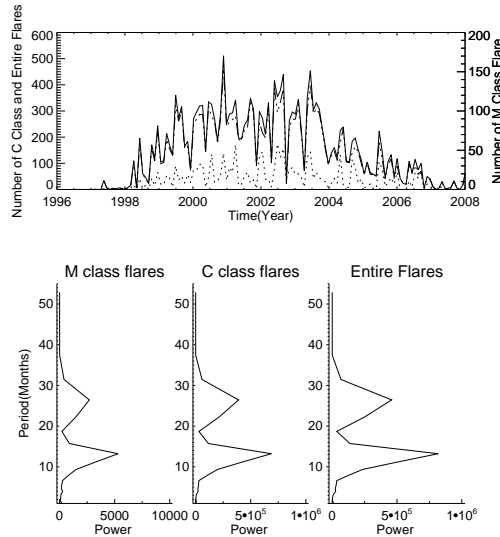


Fig. 2.— The number evolution of C class flares(dotted line), M class flares(dashed line) and all classes of flare number(solid line) above C1.0 class during solar cycle 23(upper panel), and the power spectra of flare occurrence obtained by wavelet analysis (lower panel).

in 402), γ (100%, 1 in 1) and $\gamma\delta$ (83%, 5 in 6) (upper panel). For these regions containing the listed configurations, the M class flare productivity reached 28%(11 in 39) in the active regions containing configurations of $\beta\delta$ producing 18 M class flares; 10%(102 in 1033) in regions of $\beta\gamma$ hosting 139 M class flares; 34%(138 in 402) in regions of $\beta\gamma\delta$ inducing 256 M flares, and for rare configurations, 100%(1 in 1) productivity in the region of γ and 50%(3 in 6) in regions of $\gamma\delta$. Finally for X class flare production, the highest efficiency took place in active regions containing configurations of $\beta\gamma\delta$ hosting 46 X class flares by 38 of 402 regions, with productivity of only 9%; and 8% in those of $\beta\delta$ producing 4 X class flares. This statistics reveals the conclusion that energetic flares are not only relatively favored regions classified $\beta\gamma\delta$ (Sammis et al., 2000) but also more configurations relatively. But the absolute productivity is not so high for those regions hosting more than 10 energetic flares. A similar conclusion has been drawn by Ternullo et al. (2006) but with a shorter time span in the cycle.

On the other hand, detectable variations of configuration can reveal another way to get the flare production efficiency.

In the top panel of Fig.4, we plot the productivity of 13 magnetic configuration evolution patterns among 31 patterns during the cycle. These patterns are selected by the criterion that the number of active regions that underwent one of these evolutions is more than 9. In the bottom panel is illustrated the number of corresponding active regions. It should be noted that some active regions could experience several evolution patterns. The symbol ' \diamond ' indicates the productivity including all flares above class C1.0, while the symbol ' Δ ' stands for the productivity for M class flares and symbol '*' for X class flares. The highest productivity (75%) of flares of all classes involves the evolution from $\beta\gamma$ to α , though the most frequent configuration change pattern was from α to β . In fact, there are 6 important evolution patterns that show very high productivity (above 55%). They are $\beta\delta \rightarrow \beta$, $\beta\gamma \rightarrow \alpha$, $\beta\gamma\delta \rightarrow \beta$, $\beta\gamma \rightarrow \beta$, $\beta\gamma \rightarrow \beta\gamma\delta$ and $\beta\gamma\delta \rightarrow \beta\gamma$. On the other hand, the M or X class flares were not highly favored by any those 13 kinds of active regions. The highest M class flare productivity (33%) occurred in the regions experiencing evolution from $\beta\gamma$ to α , and only 10 M class flares were produced in 4 regions. It was also this evolution pattern which contained the highest X class flare rate of production among the 13 evolution patterns. 2 among 12 of such regions produced 5 X class flares with a productivity of 17%. The relatively high M class productivity occurs in the evolution patterns from $\beta\delta\gamma$ configuration to other configurations. For instance, 33%(1 in 3) in the regions of configurations from $\beta\delta\gamma$ to α , 30%(16 in 53) to β , 33%(3 in 9) to $\beta\delta$, 50%(1 in 2) to $\beta\gamma$. And finally 30%(36 in 118) from $\beta\delta\gamma$ to $\beta\gamma$.

For very rare evolution patterns, like that from γ to $\beta\gamma\delta$, 100% M class productivity has been reached but only one active region once experienced such evolution. However, the very

low X class flare production rate was evidenced for the most frequently evolution patterns. The rate of production is only 12.5% (1 in 8 regions) obtained by the evolution from $\beta\delta$ to $\beta\gamma\delta$ and 11%(1 in 9 regions) from $\beta\delta$ to $\beta\gamma$.

3. One Way to Give Short-term Prediction of Solar M and X Class Flares

In the above analysis, we see the statistical correlation of the Hale classification and its evolution to flare productivity obtained from solar cycle 23. Evidently, some specific configurations and evolutions of active regions have very high flare production efficiencies. However, for M and especially X class flares (which are significant for the prediction), we did not see enough high productivity (say, above 50%), with enough flares, by observing the magnetic features of active regions. Naturally, one always expects to forecast more individual energetic flares. Therefore, to get a valuable and accurate warning, one should search more determinant features for those active regions hosting energetic flares.

One way is to consider the real time measurable kinetic features of sunspots among which two features, to our knowledge, are good choices, i.e., the emergence of new flux (Li et al., 2007) and rotation of the sunspots (Yan et al., 2007) . Here, we focus on the latter, and try to analyze the energetic flare productivity of active regions having sunspot rotations of different types, along with their magnetic configurations.

During solar cycle 23, 182 rotating sunspots from December 1996 to December 2007 were found (Yan et al., 2008a). Among them, 35 X class flares were related to 17 active regions with their sunspots rotated before flare occurrence. The rotation causes the energy accumulation of the flare (see Yan et al., 2007). By tracing the rotation and the following flare occurrence, we give the statistical analysis of the correlation between flares and rotations. In our recent research (Yan et al., 2008b), sunspots with rotations are classified into several types related to their magnetic configurations and the productivity was listed.

Figure 5 illustrates the time difference between the recognizable start time of rotation and the onset time of X class flares. It should be pointed out that the start time of sunspot rotation depends on the data sources (Yan et al., 2008b), typically the error is about 2 hours. One can see from the figure that the smallest time difference is a little longer than 2 hours while the greatest difference is less than 150 hours (a little longer than 6 days), which happened for type Vb. On the other hand, some of these regions produced more than one flare, and the time difference between successive flares within the same region can also be seen from the figure. The definition of these rotation types related to the magnetic configuration can be found in Yan et al.(2008b).

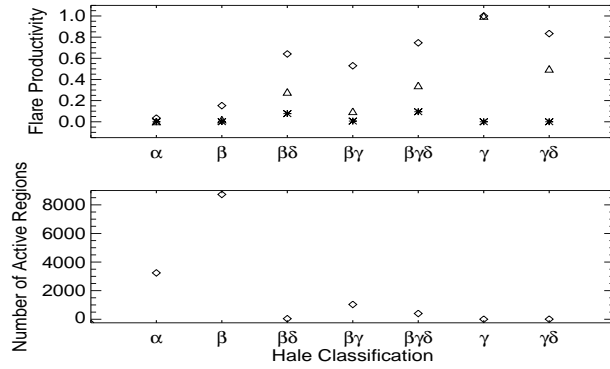


Fig. 3.— The flare productivity of different magnetic configurations (upper panel) and the numbers of these active regions of corresponding types (lower panel). The symbol ' \diamond ' represents the productivity for all classes of flare while ' \triangle ' for M class flares and '*' for X class.

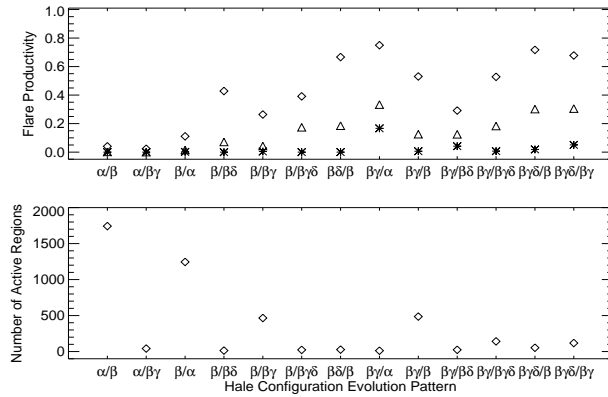


Fig. 4.— The flare productivity of different magnetic configuration evolution patterns (upper panel) and the numbers of these active regions (lower panel). The symbol ' \diamond ' represents the productivity for all classes of flare while ' \triangle ' for M class flares and '*' for X class.

From the statistics, the energetic M and X class flare productivity can reach 100% in active regions of special types. For instance, in those active regions with rotating sunspots and magnetic configurations of type Vb (NOAA10930, NOAA09236, the only two regions found belonging to the type in the cycle), there were 5 X class flares occurring in the two regions. For M class flares, 100% production efficiency was met by types IVc, IVd and Vb. 5 M class flares occurred in NOAA09070 of type IVc, 1 M class flare happened in NOAA10464 of type IVd, 9 M flares took place in NOAA10930 and NOAA09236 of type Vb. Therefore, active regions of type Vb are very productive with respect to energetic flares! This type of active region was defined as follow: in these regions there is one sunspot that not only spins but also rotates around another sunspot with opposite polarity(Yan et al.,2008b).

Other types of rotation patterns which exist in the active regions can also induce high production rates of M and X class flares. For instance, for M class flare, types IIa, IIIa, IIIb, and VIb can have more than 66% productivity. In detail, 6 in 8 active regions of type IIa manufactured 42 M class flares, with productivity of 75%; 5 in 6 active regions of type IIIa gave birth to 31 M class flares and 5 in 6 regions of type IIIb produced 42 M class flares with the same productivity of 83%; 2 in 3 regions of type VIb induced 8 M class flares, with productivity of 67%.

Therefore, we conclude that, if the measurable kinetic features of sunspots in active regions are taken into account, one may obtain a very high reliability for energetic flare prediction.

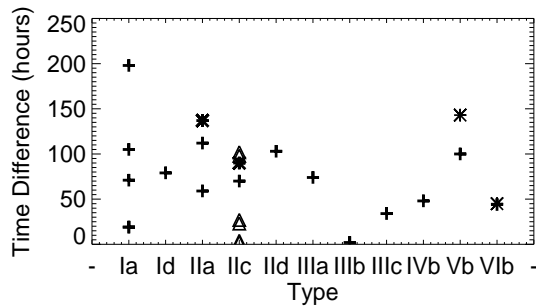


Fig. 5.— Time difference between the detectable beginning time of sunspot rotation and the onset of X class flares. In the diagram, for the same type of rotation in the vertical direction, different symbols indicate different active regions.

4. Conclusions

Evidently, the most difficult mission for solar physicists is to forecast flares far from sunspot-inhabited regions. However, in active regions, one can find some clues to issue even short-term predictions of individual flares as we provided in the above section. At the present stage, researchers cannot give exact short-term predictions for all individual solar flares. Therefore, one way is to issue predictions with high reliability.

In this paper, we find C and M class flare occurrence periods of 13.2 months occurring twice during solar cycle 23 and we believe that such activity periodicity may exist in the past cycles or the coming cycles. This can be used for medium-term forecasting. Additionally, some special magnetic configurations and their evolution patterns can also help us present short-term prediction. They are listed as follows:

1) Magnetic configurations. Usually, the more complicated are the configurations of the active regions, the higher the productivity they have. For all kinds of flare classes, configuration $\beta\gamma\delta$ has the highest rate of production, followed by $\beta\gamma$;

2) Magnetic configuration evolution patterns. The flares are favored by evolution patterns from configuration $\beta\gamma\delta$ to other ones.

However, as pointed out above, one cannot get high reliability for predicting energetic flares by only observing the two dimensional magnetic configurations and their evolutions. But we also showed that it is possible to make short-term predictions with high reliability of more individual energetic flares if the real time measurable kinetic features of active regions, like sunspot rotation, are taken into account. Especially, we listed the sunspot rotation patterns of active regions related to magnetic configurations that showed high productivity of energetic flares as follows:

1) High X class productivity. Active regions having sunspot rotation type Vb(100%);

2) High M class productivity. Active regions having sunspot rotation types IVc, IVd, and Vb have 100% productivity and active regions of types IIa, IIIa, IIIb, and VIb have production rates above 66%.

The features of active regions having 100% M or X class flare productivity are candidates for the sufficient conditions we are searching for. Other features with high productivity, e.g., above 66%, are also very useful. Of course, more real time measurable features can be included, for instance, the emergence of new flux into the active regions (Li et al., 2007). Therefore, it is reasonable to expect that more and more energetic flares can be predicted. On the other hand, one can also consider the WTD for these specific individual regions, like the work done by Wheatland(2001). It is evident that combining these two methods will

promote short-term prediction for more and more individual flares.

Finally, it should be pointed out that the productivity of the above specified types of active regions may experience fluctuations from one cycle to another. However, our work here provides some clues or methods to promote medium- and short-term flare prediction.

Acknowledgments This work is supported by the National Science Foundation of China (NSFC) under the grant number 10673031 and 40636031, National Basic Research Program of China 973 under the grant number G2006CB806301. The authors are grateful to the BBSO, TRACE, SOHO/MDI and HINODE consortia etc. for their data.

REFERENCES

- Atac,T., 1987, Ap&SS, 129, 203
- Cui Yanmei, Li Rong, Wang Huaning and He Han, 2007, Solar Phys., 242, 1
- Cui Yanmei and Wang Huaning, 2007, Adv. Spa. Res. 42, 1475
- Gallagher,P.T., Moon, Y.-J., Wang, H., 2002, Solar Phys., 209,171
- Greatrix,G.R., 1963, MNRAS, 126,123
- Jakimiec,M. and Bartkowiak,A. 1994, Acta Astronomica, 44, 115
- Li,H., Schmieder,B., Song,M.T., and Bommier, V., 2007, A&A, 475, 1081
- Mayfield,E.B. and Lawrence,J.K., 1985, Solar Phys., 96,293
- Qahwaji, R. and Colak, T., 2007, Solar Phys., 241, 195
- Sammis, I., Tang, F. and Zirin, H., 2000, ApJ, 540, 583
- Tandberg-Hanssen, E., Emslie, A.G., 1988, *The physics of solar flares*, Cambridge University Press
- Ternullo, M., Contarino,L., Romano, P. and Zuccarello F., 2006, Astron. Nachr. 327, 36
- Yan, X.L., Qu, Z.Q. and Xu, C.L., 2008, ApJ, 682, L65
- Yan, X. L., and Qu, Z. Q., 2007, A&A, 468, 1083
- Yan, X.L., Qu, Z.Q. and Kong, D.F. , 2008, MNRAS, to be published

Zhu Cui-lian and Wang Jia-Long, 2003, *Chin.J.Astron.Astrophys.*, 3, 563